Collagen Remodeling Plays a Pivotal Role in Endothelial Corneal Dystrophies

Marcus Walckling,[1] Rica Waterstradt,[2] and Simone Baltrusch[2,3]

[1]Department of Ophthalmology, University Medicine Rostock, Rostock, Germany
[2]Institute of Medical Biochemistry and Molecular Biology, University Medicine Rostock, Rostock, Germany
[3]Department Life, Light & Matter, University of Rostock, Rostock, Germany

Correspondence: Simone Baltrusch, Institute of Medical Biochemistry and Molecular Biology, University Medicine Rostock, Schillingallee 70, 18057 Rostock, Germany; simone.baltrusch@med.uni-rostock.de.

Received: July 6, 2020
Accepted: November 6, 2020
Published: December 1, 2020

Citation: Walckling M, Waterstradt R, Baltrusch S. Collagen remodeling plays a pivotal role in endothelial corneal dystrophies. *Invest Ophthalmol Vis Sci.* 2020;61(14):1. https://doi.org/10.1167/iovs.61.14.1

Purpose. To elucidate the collagen structure in the Descemet membrane (DM) of the human cornea and to characterize its rearrangement in patients with endothelial corneal dystrophies.

Methods. Corneas from nine human donors and dystrophic DMs removed from 16 affected eyes of 13 patients by endothelial keratoplasty (DMEK) were investigated using a correlative RT-qPCR and label-free two-channel multiphoton microscopy (MPM) setup. Although collagen formation was visualized by second harmonic generation, the cellular structure was determined by autofluorescence.

Results. The DM of the human donor cornea was characterized by a consistent pattern of fine hexagonal collagen structures that form a supportive scaffold for the endothelial cells. Accordingly, network-forming collagens (8A1 and 8A2) but less fibrillar collagens (only 1A2) were expressed. DMEK resulted in significant ($P < 0.0001$) improvement of best-corrected visual acuity. In the removed dystrophic DMs, MPM analyses revealed collagen rearrangement in addition to loss of endothelial cells and the development of guttae. MPM analyses of the whole patient's DM demonstrated this collagen remodeling in its entirety and facilitated correlation to Scheimpflug corneal tomography. In most DMs a unique honeycomb collagen network was identified, with distinct bundles surrounding the guttae and correlating with expression of fibrillar collagens (1A1). Conversely, some DMs showed either reduced collagen on MPM and RT-qPCR analysis or diffuse thickening and storage of extracellular matrix.

Conclusions. The collagen structure of the DM and its adaptive remodeling in endothelial corneal dystrophies has been characterized for the first time here and will facilitate individual therapeutic approaches.

Keywords: Descemet membrane, endothelial corneal dystrophies, guttae, Descemet membrane endothelial keratoplasty, multi-photon microscopy, second harmonic generation, autofluorescence, collagen remodeling, network-forming collagens, fibrillar collagens

The corneal endothelium is a monolayer of cells that is attached to the Descemet membrane (DM) and regulates fluid and solute transport between the aqueous humor and the corneal stroma. The collagen fiber and extracellular matrix glycoprotein composition of the DM is still not fully understood, but fibrillar collagens (type 1 and 5),[1] basement membrane collagen (type 4),[1] network-forming collagen (type 8),[2] as well as laminins and fibronectins and elastic fibers[3] have been proposed. Aging adversely affects DM thickness and elasticity, as well as endothelial cell density,[4–6] although the latter seems to be compensated by stretching of remaining cells.[7] Because these cells do not regenerate naturally, their loss entails stromal fluid imbalance, eventually leading to corneal edema and progressive vision loss.

Almost always, diagnosis of such disorders by slit-lamp examinations reveals endothelial droplet-like excrescences (guttae). However, in the category of endothelial pathologies, Fuchs endothelial corneal dystrophy (FECD) and pseudoexfoliation syndrome (PEX)[8] both display a wide variety in terms of clinical presentation.[9–13] While the more common FECD is limited to the endothelial layer and becomes symptomatic earlier with a higher prevalence in women, patients with PEX also have fibrillar deposits in other tissues and suffer from reduced vision later in life.

Genetic linkage analyses and recent genome-wide association studies have provided strong evidence to support a genetic predisposition for both conditions.[14,15] To date, in the rare early-onset subtype of FECD, only inherited genetic polymorphisms in the COL8A2 gene have been identified and phenotypically related to abnormal assembly and accumulation of the encoded type 8 collagen, a major component of the DM.[15–18] In the more common late-onset subtype of FECD, in contrast, associations have been found with other genes in addition to COL8A2.[15] Polymorphisms in the transcription factor 4 (TCF 4) gene, and especially an intronic Cytosine Thymine Guanine (CTG) trinu-

Copyright 2020 The Authors

This work is licensed under a Creative Commons Attribution-NonCommercial-NoDerivatives 4.0 International License.

cleotide repeat expansion, have been most frequently identified in Caucasian FECD patients.[19–21] However, the pathophysiology of FECD and PEX in the elderly often remains unknown.[22–26]

Thus correlation of genetic analyses and of clinical outcomes with morphologic changes in the DM represents a major step forward in understanding the pathophysiology of corneal endothelial dysfunction.[17,27] Both scanning and transmission electron microscopy analyses have provided general structural information about the human cornea.[28–30] However, sectioning of the posterior stroma and its differentiation from the DM on the basis of observed electron microscopy patterns remains controversial.[31,32] Whereas the outcome of electron microscopy studies is limited by relatively rigid sample preparation, multi-photon microscopy (MPM) can be applied under native conditions while maintaining the fluid homeostasis of the cornea.[33–37]

Over the last decade Descemet membrane endothelial keratoplasty (DMEK) has become the standard treatment in many countries for patients suffering from corneal endothelial dysfunction.[38–40] The present study uses MPM to compare DMs from corneal dystrophy patients with no family history of FECD who have undergone DMEK with healthy DMs from donor eyes. Full high-resolution three-dimensional (3D) images have the potential to reveal different stages of collagen rearrangement, extracellular matrix formation and endothelial cell structure as a function of aging and pathology. Finally, collagen expression in the samples and ex vivo findings will be correlated with patient history and diagnostic outcomes.

Methods

This study was approved by the Rostock University Medicine Ethics Review Board and adheres to the tenets of the Declaration of Helsinki. Altogether 13 patients with endothelial disorders who underwent DMEK surgery at the Department of Ophthalmology, Rostock University Medicine were included. Removed DMs were stored in corneal culture medium (Merck K2 medium, F9017, supplemented with 2.5% fetal calf serum) and analyzed blinded with respect to the clinical investigations. Residual human donor corneal sections (epithelium and stroma after DM preparation, n = 7) and corneas (because of cancellation of surgery at short notice, n = 3) with approval for research were obtained from the German Society for Tissue Transplantation (DGFG) in corneal culture medium.

Clinical Examinations

All patients underwent complete ophthalmological examination before and after surgery, including slit-lamp biomicroscopy and Scheimpflug tomography (Pentacam; Oculus, Wetzlar, Germany). Tomographic maps of corneal thickness were generated using Pentacam software (Version 1.21r43). In addition, central corneal thickness (CCT) and corneal anterior and posterior surface wave front higher-order aberration (HOA) at the 6 mm optical zone were calculated. Best-corrected visual acuity (BCVA) was determined with reference to the logarithm of the minimum angle of resolution (LogMAR). Intraocular pressure (IOP) was measured by Goldmann applanation tonometry. Final differential diagnosis of FECD and PEX, and in one case of bullous keratopathy (BK), are based on appearance of corneal guttae and endothelial decompensation.[41] In addition, full patient histories were taken, and a family history of corneal diseases was excluded.

DMEK Surgery

DMEK was performed under local parabulbar anesthesia or general anesthesia as described previously.[38] Immediately before the operation, the donor DM was prepared. Air was supplied to the anterior chamber. Descemetorhexis of 8 mm diameter was performed. The DM was not discarded as usual, but immediately transferred into a tube with corneal culture medium and stored at room temperature. Current bridges were removed using an I/A handpiece. The donor DM was picked up by a glass cartridge, implanted and unfolded. A 20% SF6 gas bubble was introduced under the DM. Subsequently, the eye was inflated with balanced salt solution, and the ports were sealed by hydration.

Multiphoton Microscopy

All samples were analyzed in corneal culture medium at least 24 hours after surgery using an upright dual-line FVMPE-RS multiphoton microscope (Olympus, Hamburg, Germany) equipped with a femtosecond laser system (InSight DS Dual-OL; Spectra-Physics, Santa Clara, CA, USA).[36,37] A galvanometer scanner with 512 × 512 pixel was used with scan times of two to eight seconds per pixel. Images sized 512 × 512 to 2048 × 2048 were acquired with an XLPLN25xWMP (NA 1.05) objective at zoom 1.0 to 4.0 and cooled gallium arsenide phosphide photo-multiplier tubes. The 3D images were obtained by depth serial recordings with a step size of 0.5 to 2.0 µm. Sequential line scan was applied for dual-channel imaging with DM 690 and LCDM 1030-13 filters. Autofluorescence was detected with a 740 nm excitation wavelength (tunable laser line) and a BA460-500 emission filter; second harmonic generation (SHG) was detected with a 1040 excitation wavelength (fixed laser line) and a BA520-560 emission filter. Whole sample maps were generated by multi-area time-lapse imaging. Final images were generated by Imaris software (Oxford Instruments/Bitplane, Zurich, Switzerland).

Gene Expression Analysis

DMs and corneal sections were homogenized in QIAshredder Mini Spin Columns (Qiagen, Hilden, Germany) by centrifugation (2 minutes, 12,000 rpm). Thereafter RNA was isolated and purified with the RNeasy Mini Kit (Qiagen). The cDNA was synthesized using the Maxima First Strand cDNA synthesis kit for RT-qPCR (Thermo Scientific, Darmstadt, Germany). RNA solutions containing the probes of the cDNA synthesis kit were placed in a thermocycler (Labcycler; SensoQuest, Göttingen, Germany) programmed at 25°C for 10 minutes, followed by 50°C for 15 minutes and by 85°C for five minutes. For real-time PCR, cDNA solutions containing TaqMan Universal Master Mix (Applied Biosystems, Darmstadt, Germany) and one of the following TaqMan Gene Expression Assays (Col1A2 HS 01028956_m1, Col1A1 HS 00164004_m1, Col4A1 HS 00266237_m1, Col4A2 HS 05006309_m1, Col5A1 HS 00609133_m1, Col5A3 HS 01555669_m1, Col8A1 HS 00156669_m1, Col8A2 HS 00609133_m1, CryAB Hs00157107_m1; Applied Biosystems) of primer and gene probe were amplified and detected using a 7900HT Fast Real-Time System (Life Technologies,

Investigative Ophthalmology & Visual Science

Darmstadt, Germany). The PCR system was programmed at 50°C for two minutes, followed by 95°C for 10 minutes and by 100 repeats of the steps 95°C for 15 seconds and 60°C for one minute. Selection of an endogenous control for normalization was done in line with the TaqMan Gene Expression (Applied Biosystems) recommendations. The coefficient of variation of the C_t values was 2.6% for GAPDH (Hs02758991_g1), 5.2% for Actin (Hs01060665_g1), 3.8% for PPIA (Hs04194521_s1), and 4.4% for RPL5 (Hs03044958_g1) in the three human donor corneas. Finally, with its relatively constant expression level, GAPDH served as a housekeeping gene in this study. Gene expression values were calculated with the SDS RQ Manager 1.2 software (Life Technologies).

Statistical Analysis

Results are presented as means ± SD. Statistical analyses were performed using the Prism 8 analysis program (GraphPad, San Diego, CA, USA). Differences were examined using unpaired *t* test, Mann-Whitney test or one-way ANOVA with Bonferroni's multiple comparisons test as indicated and *P* values <0.05 were considered to be statistically significant. Correlations were evaluated using the Pearson correlation coefficient.

Results

Corneal Findings in DMEK Patients

Altogether 16 eyes of 13 patients (8 female/5 male with mean age 66 ± 13 years) were analyzed. Twelve eyes were pseudophakic, one eye was aphakic, and three eyes were phakic before and pseudophakic after Triple-DMEK. Final diagnosis was FECD for 11 eyes, PEX for three eyes, BK for one eye, and endothelial pathology for one eye (Table). Patients with early onset FECD or a family history of FECD were not included in this study. Mean BCVA (LogMAR) was 0.58 ± 0.09 before DMEK and improved significantly ($P < 0.0001$) to 0.17 ± 0.07 at three months after surgery. Mean IOP was 12 ± 2 mm Hg preoperatively and 14 ± 3 mm Hg after surgery; mean CCT was 647 ± 64 µm before surgery and decreased significantly ($P < 0.0001$) to 514 ± 37 µm after surgery; age dependency of CCT was absent before surgery (Pearson's *r*: −0.044) but was present after surgery (−0.41); mean anterior HOA was 0.692 ± 0.280 before and 0.871 ± 0.327 after surgery; mean posterior HOA was 0.447 ± 0.233 before surgery and decreased significantly ($P = 0.0284$) to 0.291 ± 0.093 after surgery (Table; excluding patients with BK and not detected values).

Structure and Gene Expression of Human Donor Cornea

Residual human donor corneal sections (7.5 mm diameter) after DMEK preparation consisted of epithelium and stroma, as displayed by cellular autofluorescence and the collagen SHG signal on MPM (Fig. 1A). Gene expression analyses of seven corneal sections (mean age 73 ± 7 years) revealed the presence of different collagen types, with the significantly highest values found for 1A1 and 1A2 (Fig. 1B). Three human corneas (ages 51, 66, and 76 years) were investigated by MPM (Figs. 1C and 1D; Figs. 2 and 3) before the endothelium attached to the DM was removed from the stroma (Fig. 1H). The margin of the preparation shows the trabecular meshwork (Fig. 1E). After imaging, gene expression of the endothelium was considered in comparison to epithelium and stroma (separated from residual sclera). Although expression of collagen types 1A1 and 5A1 was absent, that of 8A1 was significantly higher and that of 8A2 was higher (Fig. 1G). In addition, crystallin AB was detectable in the corneal preparations with significantly higher gene expression in the endothelium than in stroma and epithelium (Fig. 1I).

The lateral SHG image of the 51-year-old cornea revealed collagen texture that changed in density between the epithelial and endothelial border (Fig. 1C). Dual-channel imaging of SHG and autofluorescence displayed Bowman's membrane as the interface between epithelium and stroma in further detail (Fig. 1D). Likewise, the DM as the interface between endothelium and stroma exhibited diffuse autofluorescence surrounding the distinctly cellular structure (Figs. 3A left and 3B). Interestingly, SHG imaging of that precise location revealed a consistent pattern of fine hexagonal structures (Figs. 2A–2C; Fig. 3A middle) that differed from the attached stroma in both collagen texture (Figs. 2D–2F) and density (Fig. 2G). Endings of the DM collagen appeared to anchor endothelial cells (Fig. 3A right), also detectable in the 76-year-old cornea (Fig. 3C). However, the hexagonal collagen structure of the DM detected in this cornea was less consistent, with areas of thickening, discontinuity and thinning (Figs. 3D, 3E). Similar findings were observed in a 66-year-old cornea (Figs. 3F, 3G).

Structure of DMs Removed from DMEK Patients

DMs removed from DMEK patients were investigated in their entirety by MPM (Fig. 4) or analyzed after imaging of central and peripheral regions by MPM with RT-qPCR (Figs. 5–8). Mapping of two DMs revealed guttae reflected by autofluorescence that was distributed nasally to temporally across the entire DM (Fig. 4C) or was localized centrally (Fig. 4G). These findings were obtained in one patient each classified with PEX (Fig. 4A) and FECD (Fig. 4E), respectively. Both corneas improved to a more physiological thickness pattern after surgery (Figs. 4B and 4F). In addition, a strong signal was observed by SHG imaging. By contrast with the fine hexagonal structures found in donor DMs, collagen bundles surrounding the guttae formed a network with high (Figs. 4C and 4D) or medium density (Figs. 4G and 4H).

In further analyses, DMs were grouped by gene expression of collagen 1A1, 1A2, and 8A1. Those membranes that express collagen 1A1 at a significant level (unlike donor DMs) and 0.34-fold 1A2 and 0.23-fold 8A1 expression in comparison to donor DMs (Fig. 5A) showed collagen bundles (Fig. 6E). Collagen developed as single fibers filling the spaces between guttae (Figs. 5B and 5K) and forming networks partly covering the surface in central regions (Figs. 5L and 5M). Deposits are visible both in the intervening spaces and inside the guttae which often appeared with a central autofluorescence that differed from the dense cover (Figs. 5J, 5K, and 5M). The periphery showed residues of the thin hexagonal structures, seen in the donor DMs (Figs. 6A and 6C), and some endothelial cells (Fig. 6B). In the DM of a 48-year-old patient, early-stage guttae were detectable in close proximity to cells and collagen dots (Fig. 6D).

DMs that express collagen 1A2 and 8A1 at low levels and no collagen 1A1 (Fig. 7A) showed an almost dense central autofluorescence signal (Fig. 7I) with guttae (Fig. 7B) and no or only sparse collagen fibers (Fig. 7C). The membranes were thinner (Figs. 7E–7G) than those with high collagen

Investigative Ophthalmology & Visual Science

Table. Patients With Endothelial Disorders Who Underwent DMEK Surgery

DMEK	Age	Sex	Eye	Diagnosis	Lens	Pre-BCVA (LogMAR)	Post-BCVA (LogMAR)	Pre-CCT (µm)	Post-CCT (µm)	Pre-Anterior HOA	Post-Anterior HOA	Pre-Posterior HOA	Post-Posterior HOA	Pre-IOP (mm Hg)	Post IOP (mm Hg)
1L	48	f	L	**FECD**	PP	0.3	0	684	569	0.876	0.636	0.292	0.261	9	15
1R			R	**FECD**	P/PP	0.4	0.1	676	561	0.775	0.719	0.253	0.235	16	13
8	56	f	L	**FECD**	PP	0.3	−0.1	736	538	0.432	0.686	0.328	0.185	13	11
4	58	m	L	**FECD**	PP	0.3	0	654	544	0.377	0.510	0.743	0.270	11	16
3L	65	m	L	**FECD**	PP	0.4	0.1	561	497	0.948	1.487	1.077	0.435	10	18
3R			R	**FECD**	P/PP	0.5	0.1	560	515	0.547	0.633	0.488	0.304	12	16
6	68	f	L	**FECD**	PP	0.5	0.1	589	511	0.326	0.832	0.305	0.220	15	15
10	69	f	R	**FECD**	PP	0.4	0	611	454	1.358	0.685	0.595	0.484	11	5
5L	77	f	L	**FECD**	PP	0.5	0.1	594	499	0.684	0.742	0.436	0.388	13	13
5R			R	**FECD**	PP	0.4	0.1	586	480	0.401	0.872	0.351	0.222	13	11
12	78	m	L	**FECD**	PP	0.7	0.1	730	525	0.774	1.049	0.494	0.214	11	15
13	65	f	L	**PEX**	PP	1.3	0.3	647	443	0.879	1.661	0.393	0.383	7	12
7	68	m	L	**PEX**	PP	1	0.5	n.d.	520	n.d.	1.486	n.d.	0.386	10	14
2	77	f	L	**PEX**	PP	0.4	0.2	696	533	0.747	0.859	0.176	0.223	10	18
11	36	f	L	**BK**	AP	HM	1.3	1102	675	2.676	1.425	1.020	0.935	14	16
9	82	m	R	**EP**	P/PP	1.3	1	737	527	0.569	0.819	0.327	0.253	10	11

EP, endothelial pathology; AP, aphakic; PP, pseudophakic; P/PP, phakic to pseudophakic; Pre, before DMEK surgery; Post, after DMEK surgery; Anterior HOA, corneal anterior surface wave front higher-order aberration; Posterior HOA, corneal posterior surface wave front higher-order aberration; n.d., not detected; HM, hand movements.

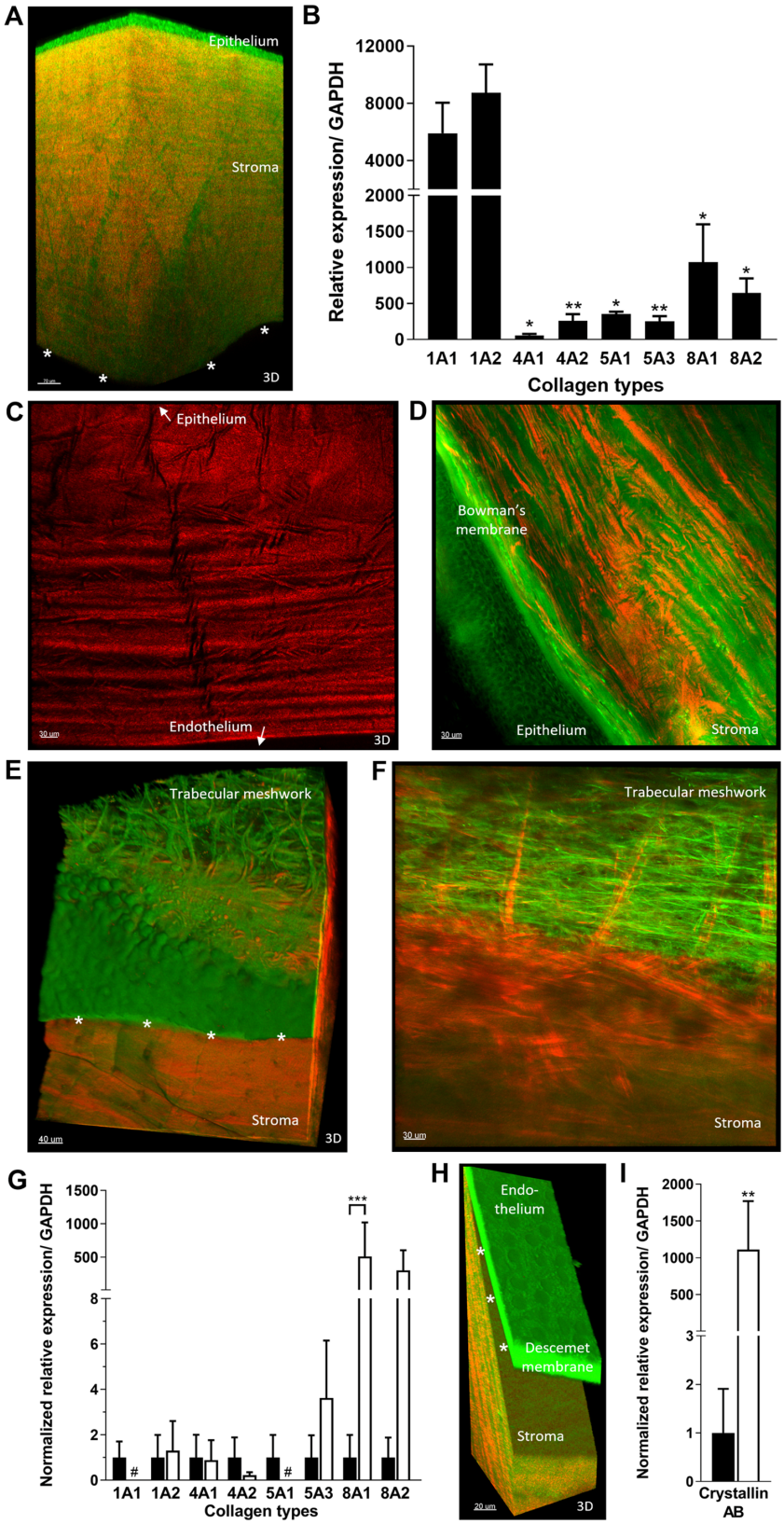

Figure 1. Collagen structure and expression in the cornea. (**A**) Residual epithelium and stroma after DMEK preparation. Preparation zone is marked by asterisks. (**B**) Relative expression of different collagen types in residual epithelium and stroma (n = 7). Data are expressed as mean ± SEM. *$P < 0.05$, **$P < 0.01$ compared to collagen 1A1 expression (ANOVA/Bonferroni's test). (**C**) Collagen structure in the stroma viewed from the side. (**D**) Bowman's membrane between epithelium and stroma viewed from the side. (**E**) Junction of the endothelium with the trabecular meshwork. Preparation zone is marked by asterisks. (**F**) Anchoring of stroma and trabecular meshwork. (**G**) Relative

Investigative Ophthalmology & Visual Science

expression of different collagen types in the endothelium (white bars) normalized to expression in epithelium and stroma (black bars) in donor corneas (n = 3). Data are expressed as mean ± SEM. *** $P < 0.001$ (ANOVA/Bonferroni's test), # $P < 0.05$ (Mann-Whitney test). (**H**) DMEK preparation was performed as marked by asterisks. (**I**) Relative crystallin AB expression in the endothelium (*white bar*) normalized to expression in epithelium and stroma (*black bar*) in donor corneas (n = 3). Data are expressed as mean ± SEM. ** $P < 0.01$ (Student's *t* test). Fluorescence signal obtained by excitation with 740 nm is shown in green and by excitation with 1040 nm in red. *Scale bars* and 3D blend projection as indicated.

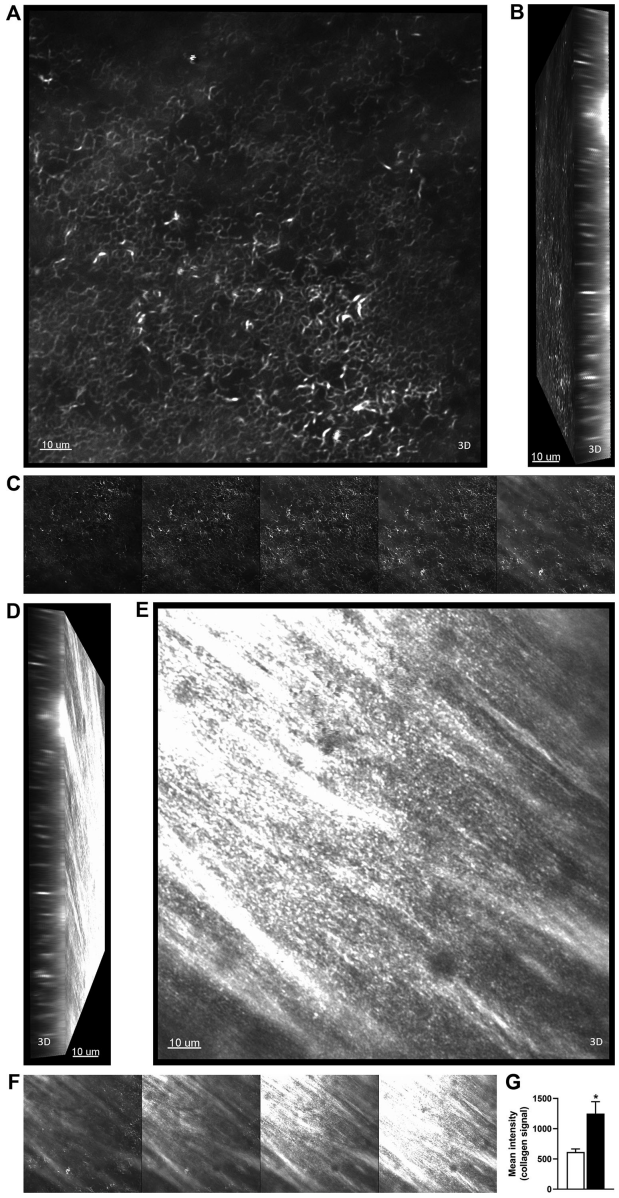

Figure 2. Visualization of DM structure in an intact 51-year-old donor cornea. Hexagonal collagen structure of DM shown in 3D blend projection (**A**), side view reconstruction (**B**) and underlying single images (**C**). Stromal collagen structure of the same area in 3D blend projection (**D**), side view reconstruction (**E**) and underlying single images (**F**). Fluorescence signal obtained by excitation with 1040 nm is shown in gray. Signal level (**G**) is significantly higher in the stroma (*black bar*) in comparison to the DM (*white bar*). Data are expressed as mean ± SEM. * $P < 0.05$ (Student's t test). *Scale bars:* 10 µm.

content (Figs. 5C–5I). Endothelial cells were detectable in the periphery and some developing guttae can be discovered at the margins (Fig. 7H).

DMs from two DMEK patients also showed low collagen 1A2 and 8A1 expression levels, but high expression of collagen 1A1 (Fig. 8A). They revealed differing structures on MPM analysis. The DM from a 36-year-old patient had a very thick autofluorescence core with a fibrous collagen cover (Figs. 8B, 8D, 8E). In contrast, that from a 68-year-old patient showed guttae in the center (Fig. 8C) and some cells in the periphery (Fig. 8G). However, a primarily fibrous extracellular network was detectable (Figs. 8F and 8G) with embedded collagen structures (Fig. 8G) also found in the sclera (Fig. 8H). Another DM showed high crystallin AB expression in particular (Fig. 8I). Together with guttae and bundled collagen (Fig. 8M and 8N), seen in most of the DMs from DMEK patients, loosely attached autofluorescence material was present that tended to exfoliation (Figs. 8J and 8L).

Discussion

MPM of the human cornea in the present study revealed significant changes in collagen arrangement, extracellular matrix formation and cell structure due to endothelial pathologies. Thus our new label-free two-channel setup proved to be useful for medical imaging of several diseases. We used a higher wavelength (1040 vs. 860 nm) than that established in the past for SHG microscopy to visualize collagen bundles. The supramolecular assembly of collagen fibers permits detection by this nonlinear optical method, and because SHG is not a resonant process, the excitation wavelength can be varied, with greater penetration depths achieved at 1040 nm. The texture of stromal collagen was shown more clearly than at the 860 nm excitation wavelength.[42] Using this approach, we have shown for the first time that the collagen structure of the DM is characterized by a consistent pattern of fine hexagonal structures. Previously such a structure has only been postulated for the endothelial cell membrane due to the presence of network-forming collagens.[26] The fine physiological structure detected appears to provide a high degree of flexibility and anchorage for the endothelial cells. In line with the hypothesis that endothelial cell loss with aging[4–6] is compensated by cell stretching, this structure showed less homogeneity in the older donor corneas. The collagen structure of the DM differs significantly from that in stroma with overlying bundles. These findings are consistent with higher expression of fibrillar collagens (types 1 and 5)[1,43] in the stroma compared with network-forming collagen (type 8)[2] in the DM.

In line with previous studies, surgery led to significant improvement with higher BCVA, and reduced CCT and posterior surface wave front HOA.[44,45] In addition, the reported age-dependent reduction in CCT was now detectable in the cohort after DMEK.[46,47] MPM analyses of

Investigative Ophthalmology & Visual Science

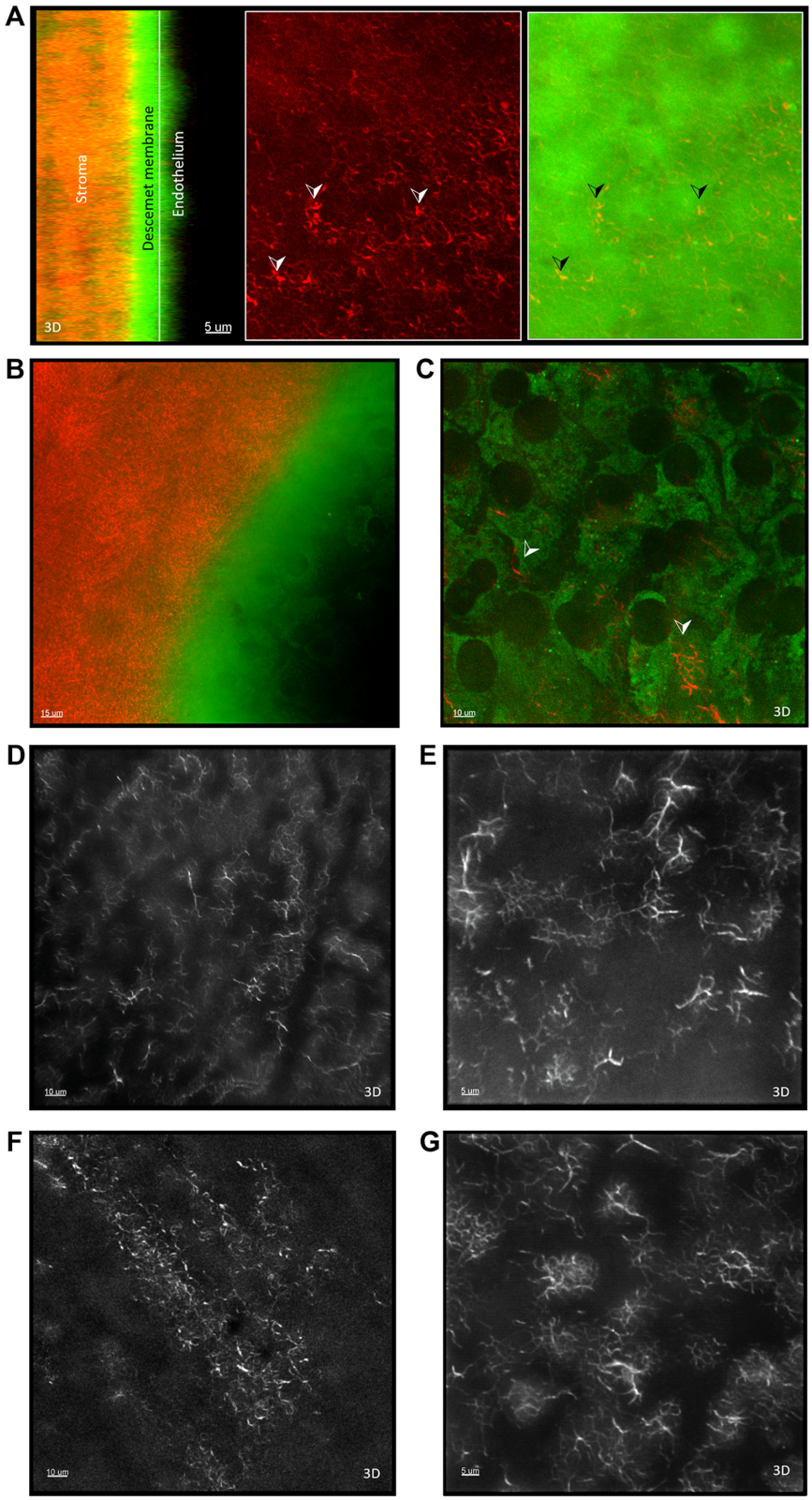

Figure 3. DM structure in intact 51-, 66-, and 76-year-old donor corneas. (**A**) Localization of DM is shown by a white line in the side view reconstruction with corresponding single images of both excitation channels. Anchoring points to cells are marked by arrow heads. (**B**) Transition from stroma to DM and endothelium viewed from the side in the 51-year-old cornea. (**C**) Endothelium and anchoring collagen (*arrow heads*) in the 76-year-old donor cornea. (**D**, **E**) Collagen structure of DM in 76-year-old donor cornea. (**F**, **G**) Collagen structure of DM in 66-year-old donor cornea. Fluorescence signal obtained by excitation with 740 nm is shown in green and by excitation with 1040 nm in red (**A**–**C**) or gray (**D**–**G**). *Scale bars* and 3D blend projection as indicated.

Investigative Ophthalmology & Visual Science

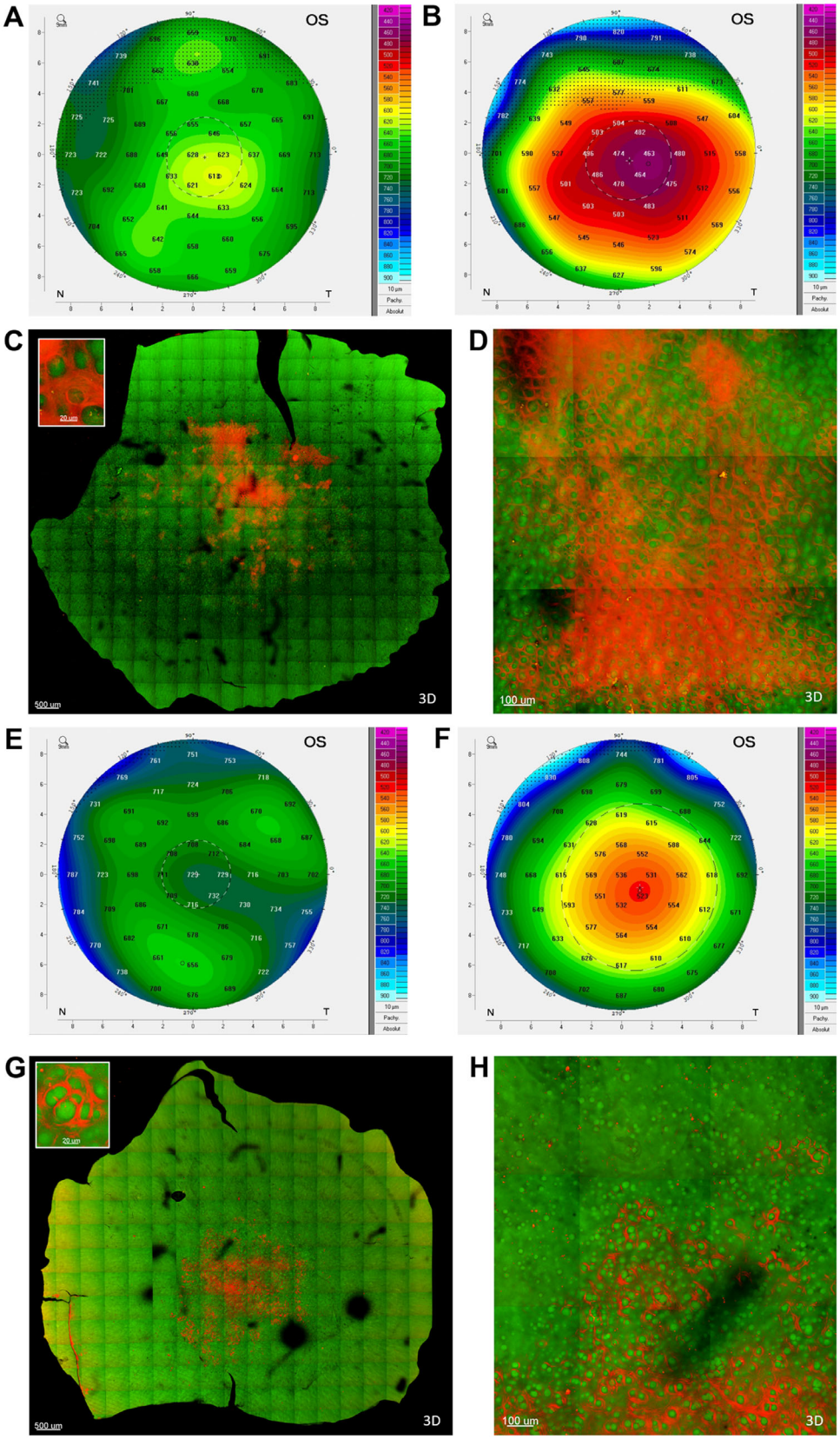

Figure 4. Tomographic maps of the cornea before and after surgery and structure of patient DMs. Pachymetry map demonstrating corneal thickness profile of DMEK 13 before (**A**) and after (**B**) and DMEK 12 before (**E**) and after (**F**) surgery. N, nasal; T, temporal. The thinnest point of the cornea is indicated by a *small circle*, and the pupil by a dashed circle with a central cross. Reconstructed map from 27,342 single images (**C**) and detail enlargements (insert **C** and **D**) from DMEK 13. Reconstructed map from 15,232 single images (**G**) and detail enlargements (insert **G** and **H**) from DMEK 12. Fluorescence signal obtained by excitation with 740 nm is shown in green and by excitation with 1040 nm in *red*. *Scale bars* and 3D blend projection as indicated.

Investigative Ophthalmology & Visual Science

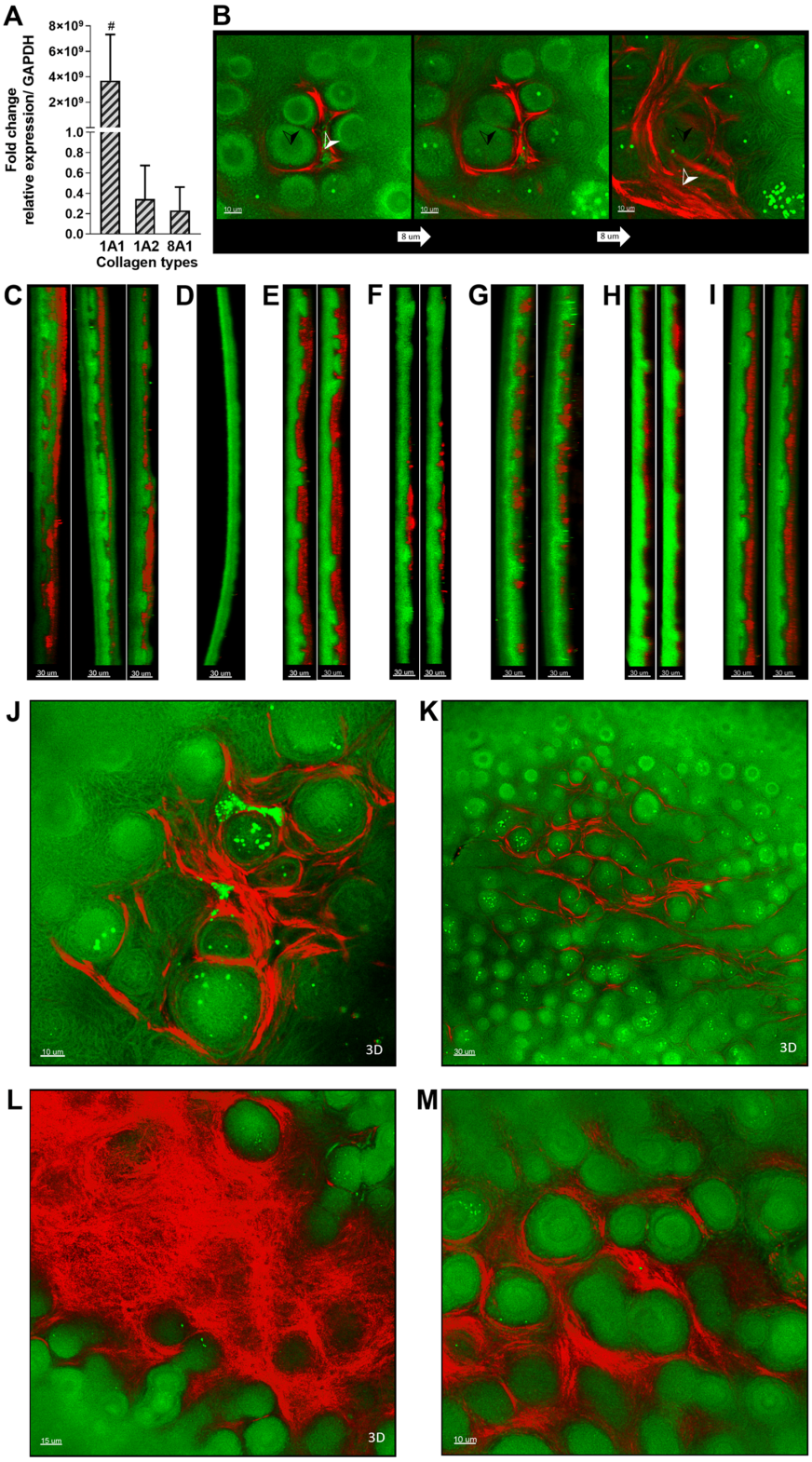

Figure 5. Structure and collagen expression of patient DMs. (**A**) Fold change in relative expression of collagen 1A1, 1A2 and 8A1 in patient DMs (DMEK 1, 5, 8, and 10, n = 4 and 6 eyes, *striped bars*) in comparison to DM of donor corneas (Fig. 1). Data are expressed as mean ± SEM. # $P < 0.05$ (Mann-Whitney test). (**B**) Single view of different layers of the same position in DM of DMEK 5R showed guttae (*black arrow heads*), deposits and collagen bundles (*white arrow heads*). Side view reconstructions of central DM of DMEK 13 (**C**), DMEK 12 (**E**), DMEK 5L (**F**), DMEK 5R (**G**), DMEK 1R (**H**), DMEK 8 (**I**), and peripheral DM of DMEK 13 (**D**). (**J, K**) Collagen bundles and deposits in DM of DMEK 5R. (**L, M**) Fibrous collagen structure in DM of DMEK 8. Fluorescence signal obtained by excitation with 740 nm is shown in *green* and by excitation with 1040 nm in *red*. *Scale bars* and 3D blend projection as indicated.

Investigative Ophthalmology & Visual Science

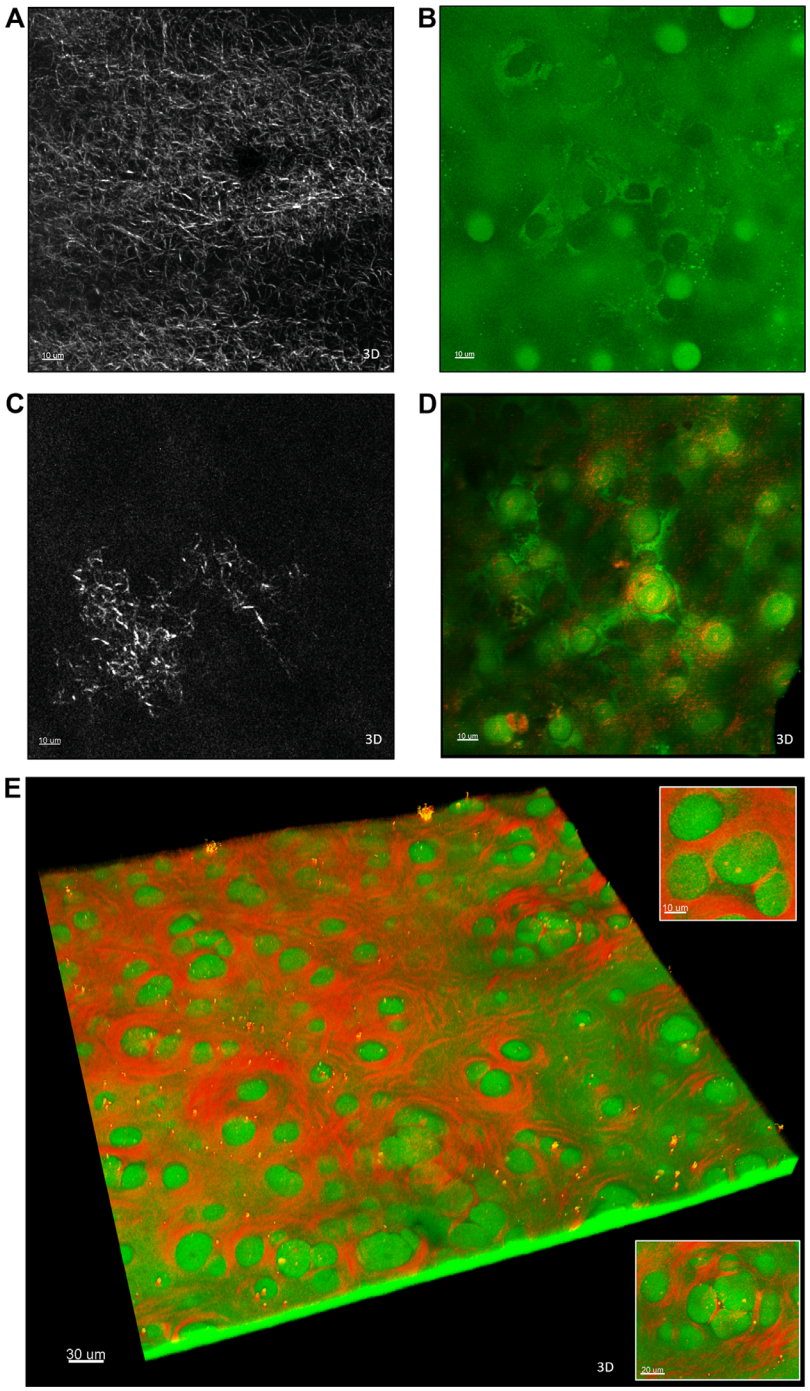

Figure 6. Development of guttae between endothelial cells in patient DMs. Different collagen structure in the periphery of DMs of DMEK 10 (**A**) and DMEK 1R (**C**). Raised guttae are visible between residual endothelial cells in the periphery of DMEK 5L (**B**). Guttae develop between cells that are partly anchored by collagen in the periphery of DMEK 1R (**D**). (**E**) Reconstruction of a central area of DMEK 12 showed a continuous collagen bundle network and a variety of guttae. Fluorescence signal obtained by excitation with 740 nm is shown in *green* and by excitation with 1040 nm in *gray* (**A** and **C**) or red (**D** and **E**). *Scale bars* and 3D blend projection as indicated.

the DMs after surgery revealed pathologic conditions not previously described. A collagen bundle network of varying intensity entwined around the guttae, primarily centrally in patients diagnosed with FECD but throughout the entire DM wherever guttae were present in patients diagnosed with PEX. Unlike other studies focusing solely on FECD,[8] we further differentiated the patients' DMs from our cohort in terms of collagen expression. With MPM those membranes expressing collagen 1A1 displayed the honeycomb collagen network and were thicker, whereas lack of collagen 1A1 expression correlated with the detected presence of marginal collagen and thinner membrane structure. Interestingly, differences between the two groups were also found in terms of patient outcome with a greater decrease in CCT after DMEK in patient DMs with abundant collagen (131 µm vs. 92 µm).

Investigative Ophthalmology & Visual Science

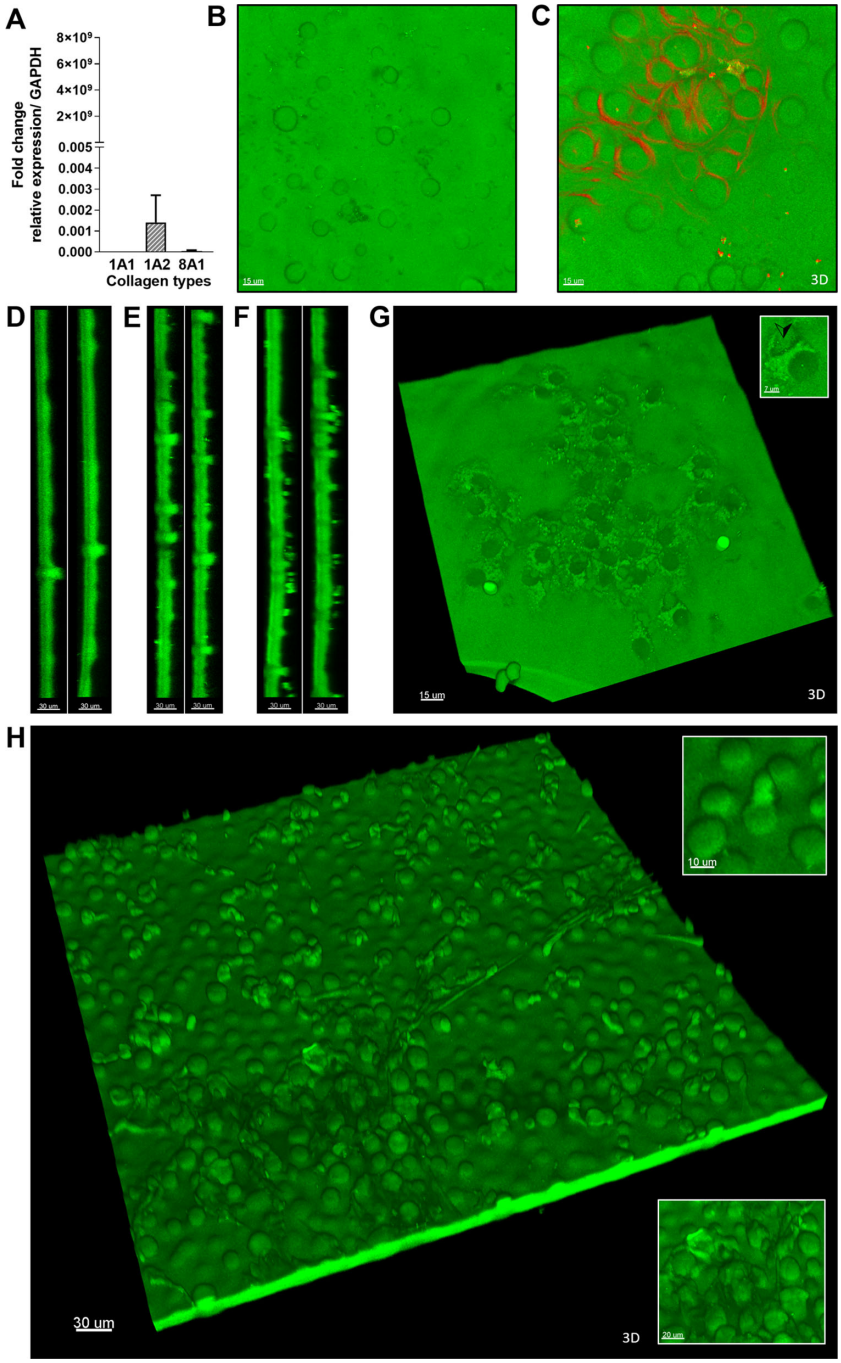

Figure 7. Collagen expression and structure of patient DMs. (**A**) Fold change in relative expression of collagen 1A1, 1A2, and 8A1 in patient DMs (DMEK 2, 3, 4, and 6, n = 4 and 5 eyes, *gray striped bars*) in comparison to DM of donor corneas (Fig. 1). Data are expressed as mean ± SEM. Guttae were detectable in all DMs, as illustrated in the case of DMEK 3L (**B**), whereas collagen was present to only a very limited degree in DMEK 3R (**C**). Side view reconstructions of central DM of DMEK 2 (**D**), DMEK 4 (**E**), and DMEK 6 (**F**). (**G**) Guttae develop between cells in the periphery of DMEK 6 (example pinpointed by a *black arrow head* in the detail enlargement). (**H**) Reconstruction of a central area of DMEK 6 showed guttae in a high-density pattern. Fluorescence signal obtained by excitation with 740 nm is shown in *green* and by excitation with 1040 nm in *red*. *Scale bars* and 3D blend projection as indicated.

We suggest that expression of fibrillar collagen and formation of the honeycomb network around the guttae are reactions of the cornea consequent on loss of the functional unit comprising the hexagonal membrane structure and endothelial cells. The pathological collagen network was found exclusively in the presence of guttae. Slit-lamp biomicroscopy examinations have demonstrated an unchanged periphery most commonly in younger patients with FECD; our description of the physiological structure of the DM corroborates that finding. However, some early-stage guttae were detectable as a result of cell death between intact cells. Second, our hypothesis is strengthened by the fact that formation of fibrillar collagen has already been described during cell growth under nonphysiological conditions and

Investigative Ophthalmology & Visual Science

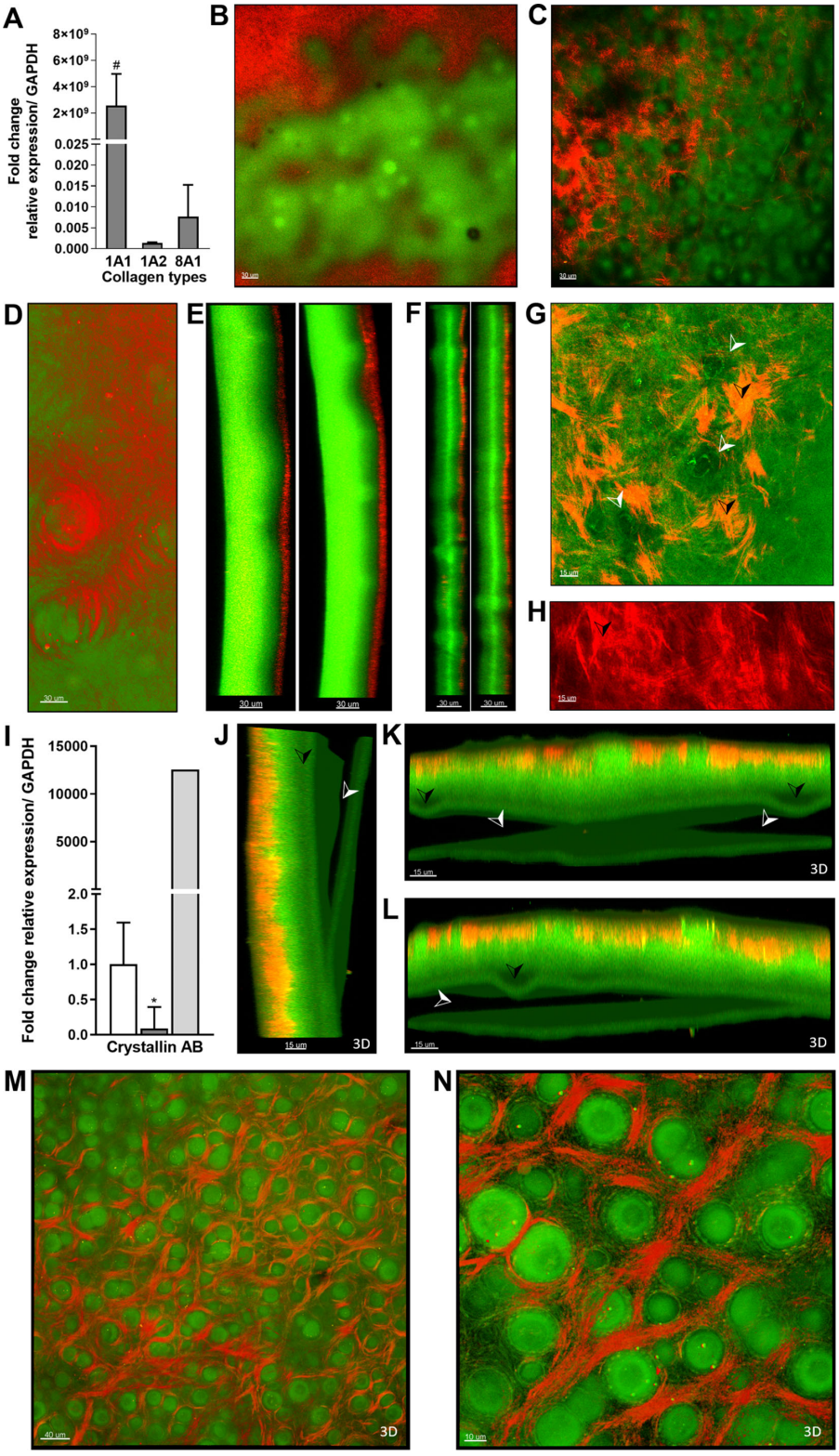

Figure 8. Collagen expression and structure of patient DMs. (**A**) Fold change in relative expression of collagen 1A1, 1A2 and 8A1 in patient DMs (DMEK 7 and 11, n = 2, *gray bars*) in comparison to DM of donor corneas (Fig. 1). Data are expressed as mean ± SEM. # $P < 0.05$ (Mann-Whitney test). Dense membrane structure with few guttae and covered by a fibrous collagen network was detectable in DMEK 11 (**B** and **D**). Collagen embedded in extracellular matrix in DMEK 7 (**C** and **G**) showed a similar pattern to that detectable in sclera (**H**). Residual endothelial cells are marked by *arrow heads* (**G**). Side view reconstructions of central DM of DMEK 11 (**E**) and DMEK 7 (**F**). (**I**) Fold change in relative crystallin AB expression in DMEK 9 (*light gray bar*) and in other patient DMs (n = 10, *dark gray bar*) in comparison to DM of donor corneas (*white bar*). Data are expressed as mean ± SEM. * $P < 0.05$ (Student's t test). Exfoliation of extracellular matrix in layers (marked by *white* and *black arrow heads*) is visible in side view reconstructions (**J–L**) of DMEK 9 that otherwise showed guttae and collagen bundles (**M, N**). Fluorescence signal obtained by excitation with 740 nm is shown in *green* and by excitation with 1040 nm in *red*. *Scale bars* and 3D blend projection as indicated.

Investigative Ophthalmology & Visual Science

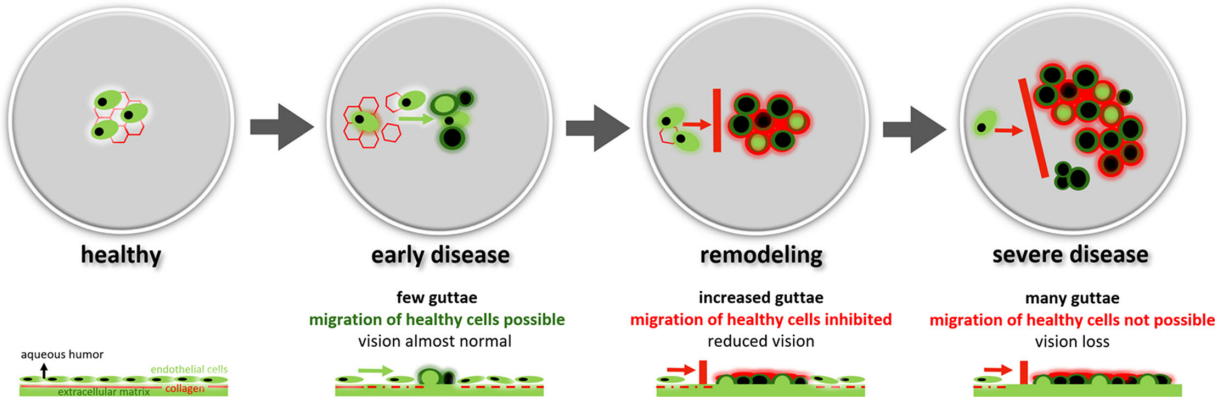

Figure 9. Remodeling of DM in endothelial dystrophies. Endothelial cells (*light green*) and the DM consisting of extracellular matrix and a collagen scaffold (*thin red hexagons and line*) form the posterior part of the cornea (*left*). In early disease (*center left*) the collagen structure of the DM is interrupted and guttae (*dark green*) develop due to cell destruction. However, healthy cells can still migrate from the periphery and DM integrity is maintained, resulting in near-normal vision. During remodeling (*center right*) increased guttae (*dark green*) initiate nonphysiological collagen production that appears as a honeycombed network (thick red structure) that inhibits the migration of healthy cells and results in reduced vision. In severe disease (*right*) numerous guttae surrounded by collagen fibers dominate the DM, rendering healthy cell migration impossible. This stage is accompanied by vision loss.

in cancer.[1,26,48–50] Although the pathological collagen rearrangement may restore corneal rigidity, the resultant impermeability and subsequent edema then become a vicious circle. We observed higher CCT values in patients developing the collagen network (648 µm vs. 612 µm) before surgery, but similar values (517 µm and 520 µm) after surgery. Interestingly, these patients showed a small but consistent improvement in corneal posterior and anterior surface wave front (HOA posterior 0.080 and anterior 0.031) after DMEK, whereas reduced collagen formation was accompanied by a greater improvement in posterior and deterioration in anterior corneal surface wave front (HOA posterior 0.267 and anterior −0.275). Our results suggest two different patterns of endothelial corneal dystrophies in terms of collagen expression.

The collagen remodeling observed in one group possibly represents a migration barrier to healthy peripheral endothelial cells, as shown schematically in Figure 9. This might explain why descemetorhexis without endothelial keratoplasty (DWEK), also known as DM stripping only (DSO), that is, removal of the centrally affected region without subsequent grafting, leads to clearing of the cornea in patients with mild to moderate FECD.[51,52] We propose that excision of the affected region opens the possibility for endothelial cells to migrate along the physiological collagen scaffold. This slow process may be reflected in the reported long recovery times in patients undergoing DWEK/DSO. However, patients with reduced collagen expression would not benefit from DWEK/DSO because of the absent interaction between DM and endothelial cells and the lost capacity for migration. Quarter-DMEK, that is transplantation of only one quarter of a donor DM, might be a useful surgical strategy in the early stages in such cases.[53] Further studies are clearly needed to elucidate whether formation of the honeycomb collagen structure depends on disease progression, individual age and corneal composition or genetic predisposition, namely the intronic CTG trinucleotide repeat expansion in TCF4.[19–21]

Three patients were differentiated from the rest on the basis of MPM imaging, which disclosed findings that were characteristic of other additional pathologies. BK was characterized not only by high CCT (1102 µm) but also by massive thickening of the DM due to an increase in extracellular matrix and the appearance of stroma-like collagen bundles. One patient with fibrosis and sclera-like collagen in the DM was suffering from secondary corneal decompensation due to severe glaucoma, having undergone multiple surgical procedures that finally damaged the cornea and introduced scleral material. Alongside the honeycomb collagen structure, one DM (from an elderly patient with occupational exposure to radiation) showed several layers of extracellular matrix with exfoliation, as confirmed by MPM. Membrane splitting has been previously described in DMEK.[28] We found higher expression of crystallin AB in the DM of this patient than in all other patients and the donor material. Crystallin AB not only plays a structural role in the lens of the eye but also serves as an important heat shock protein in several tissues. Expression of crystallin AB could be a response to UV light and radiation, resulting in loosening of the extracellular matrix of the DM and adversely affecting removal during DMEK surgery.[54,55]

MPM and RT-PCR were used to investigate DMs successfully removed from patients during DMEK surgery in comparison with healthy DMs from donor eyes. We demonstrated a consistent pattern of fine hexagonal structures, which acts physiologically to maintain the shape of the endothelial cells in the DM. Furthermore, we have provided convincing evidence that not only guttae but also collagen remodeling are participatory factors in FECD and PEX. Our results shed new light on endothelial corneal pathologies and the options available for their treatment.

Acknowledgments

The authors are indebted to David Beattie (freelance medical writer/UK) for editorial assistance in preparing the manuscript for publication and to Martin Börgel and Nicola Hofmann (German Society for Tissue Transplantation, DGFG) for support with human donor corneas.

Disclosure: **M. Walckling,** None; **R. Waterstradt,** None; **S. Baltrusch,** None

Investigative Ophthalmology & Visual Science

References

1. Kay EP. Expression of types I and IV collagen genes in normal and in modulated corneal endothelial cells. *Invest Ophthalmol Vis Sci*. 1989;30:260–268.
2. Shuttleworth CA. Type VIII collagen. *Int J Biochem Cell Biol*. 1997;29:1145–1148.
3. Feneck EM, Lewis PN, Ralphs J, Meek KM. A comparative study of the elastic fibre system within the mouse and human cornea. *Exp Eye Res*. 2018;177:35–44.
4. Laule A, Cable MK, Hoffman CE, Hanna C. Endothelial cell population changes of human cornea during life. *Arch Ophthalmol*. 1978;96:2031–2035.
5. Nucci P, Brancato R, Mets MB, Shevell SK. Normal endothelial cell density range in childhood. *Arch Ophthalmol*. 1990;108:247–248.
6. Yee RW, Matsuda M, Schultz RO, Edelhauser HF. Changes in the normal corneal endothelial cellular pattern as a function of age. *Curr Eye Res*. 1985;4:671–678.
7. Schaub F, Enders P, Zachewicz J, et al. Impact of donor age on descemet membrane endothelial keratoplasty outcome: evaluation of donors aged 17–55 years. *Am J Ophthalmol*. 2016;170:119–127.
8. Eghrari AO, Gottsch JD. Fuchs' corneal dystrophy. *Expert Rev Ophthalmol*. 2010;5:147–159.
9. Schaub F, Gerber F, Adler W, et al. Corneal densitometry as a predictive diagnostic tool for visual acuity results after descemet membrane endothelial keratoplasty. *Am J Ophthalmol*. 2019;198:124–129.
10. Sun SY, Wacker K, Baratz KH, Patel SV. Determining subclinical edema in fuchs endothelial corneal dystrophy: revised classification using Scheimpflug tomography for preoperative assessment. *Ophthalmology*. 2019;126:195–204.
11. Arnalich-Montiel F, Ortiz-Toquero S, Auladell C, Couceiro A. Accuracy of corneal thickness by swept-source optical coherence tomography and Scheimpflug camera in virgin and treated fuchs endothelial dystrophy. *Cornea*. 2018;37:727–733.
12. Patel SV, Hodge DO, Treichel EJ, Spiegel MR, Baratz KH. Predicting the prognosis of fuchs endothelial corneal dystrophy by using Scheimpflug tomography. *Ophthalmology*. 2020;127:315–323.
13. Malhotra C, Jain AK, Dwivedi S, Chakma P, Rohilla V, Sachdeva K. Characteristics of pre-descemet membrane corneal dystrophy by three different imaging modalities-in vivo confocal microscopy, anterior segment optical coherence tomography, and Scheimpflug corneal densitometry analysis. *Cornea*. 2015;34:829–832.
14. Afshari NA, Igo RP, Jr, Morris NJ, et al. Genome-wide association study identifies three novel loci in Fuchs endothelial corneal dystrophy. *Nat Commun*. 2017;8:14898.
15. Zhang J, McGhee CNJ, Patel DV. The molecular basis of fuchs' endothelial corneal dystrophy. *Mol Diagn Ther*. 2019;23:97–112.
16. Gottsch JD, Sundin OH, Liu SH, et al. Inheritance of a novel COL8A2 mutation defines a distinct early-onset subtype of fuchs corneal dystrophy. *Invest Ophthalmol Vis Sci*. 2005;46:1934–1939.
17. Gottsch JD, Zhang C, Sundin OH, Bell WR, Stark WJ, Green WR. Fuchs corneal dystrophy: aberrant collagen distribution in an L450W mutant of the COL8A2 gene. *Invest Ophthalmol Vis Sci*. 2005;46:4504–4511.
18. Kuot A, Mills R, Craig JE, Sharma S, Burdon KP. Screening of the COL8A2 gene in an Australian family with early-onset Fuchs' endothelial corneal dystrophy. *Clin Exp Ophthalmol*. 2014;42:198–200.
19. Soragni E, Petrosyan L, Rinkoski TA, et al. Repeat-associated non-ATG (RAN) translation in Fuchs' endothelial corneal dystrophy. *Invest Ophthalmol Vis Sci*. 2018;59:1888–1896.
20. Okumura N, Hayashi R, Nakano M, et al. Effect of trinucleotide repeat expansion on the expression of TCF4 mRNA in Fuchs' endothelial corneal dystrophy. *Invest Ophthalmol Vis Sci*. 2019;60:779–786.
21. Fautsch MP, Wieben ED, Baratz KH, et al. TCF4-mediated Fuchs endothelial corneal dystrophy: Insights into a common trinucleotide repeat-associated disease. *Prog Retin Eye Res*. 2020;100883.
22. Igo RP, Jr, Kopplin LJ, Joseph P, et al. Differing roles for TCF4 and COL8A2 in central corneal thickness and Fuchs endothelial corneal dystrophy. *PLoS One*. 2012;7:e46742.
23. Khuc E, Bainer R, Wolf M, et al. Comprehensive characterization of DNA methylation changes in Fuchs endothelial corneal dystrophy. *PLoS One*. 2017;12:e0175112.
24. Rao BS, Ansar S, Arokiasamy T, et al. Analysis of candidate genes ZEB1 and LOXHD1 in late-onset Fuchs' endothelial corneal dystrophy in an Indian cohort. *Ophthalmic Genet*. 2018;39:443–449.
25. Tang H, Zhang W, Yan XM, et al. Analysis of SLC4A11, ZEB1, LOXHD1, COL8A2 and TCF4 gene sequences in a multigenerational family with late-onset Fuchs corneal dystrophy. *Int J Mol Med*. 2016;37:1487–1500.
26. Weller JM, Zenkel M, Schlotzer-Schrehardt U, Bachmann BO, Tourtas T, Kruse FE. Extracellular matrix alterations in late-onset Fuchs' corneal dystrophy. *Invest Ophthalmol Vis Sci*. 2014;55:3700–3708.
27. Matthaei M, Leitl C, Cursiefen C, Heindl LM. Correlation of extracellular matrix-related gene expression with objective Fuchs endothelial corneal dystrophy severity. *Clin Exp Ophthalmol*. 2019;47:671–673.
28. Weller JM, Schlotzer-Schrehardt U, Kruse FE, Tourtas T. Splitting of the recipient's Descemet membrane in Descemet membrane endothelial keratoplasty-ultrastructure and clinical relevance. *Am J Ophthalmol*. 2016;172:1–6.
29. Cabrerizo J, Forshaw T, Rodriguez-Aierbe C, Garrido-Fierro J. Scanning electron microscopy assessment of the Descemet membrane interface during DMEK graft preparation. *Sci Rep*. 2018;8:492.
30. Xia D, Zhang S, Nielsen E, et al. The ultrastructures and mechanical properties of the Descement's membrane in fuchs endothelial corneal dystrophy. *Sci Rep*. 2016;6:23096.
31. Dua HS, Faraj LA, Said DG, Gray T, Lowe J. Human corneal anatomy redefined: a novel pre-Descemet's layer (Dua's layer). *Ophthalmology*. 2013;120:1778–1785.
32. Schlotzer-Schrehardt U, Bachmann BO, Tourtas T, et al. Ultrastructure of the posterior corneal stroma. *Ophthalmology*. 2015;122:693–699.
33. Lai T, Tang S. Cornea characterization using a combined multiphoton microscopy and optical coherence tomography system. *Biomed Opt Express*. 2014;5:1494–1511.
34. Marando CM, Park CY, Liao JA, Lee JK, Chuck RS. Revisiting the cornea and trabecular meshwork junction with 2-photon excitation fluorescence microscopy. *Cornea*. 2017;36:704–711.
35. Lombardo M, Parekh M, Serrao S, Ruzza A, Ferrari S, Lombardo G. Two-photon optical microscopy imaging of endothelial keratoplasty grafts. *Graefes Arch Clin Exp Ophthalmol*. 2017;255:575–582.
36. Baltrusch S. [Ophthalmological monitoring of diabetic neuropathy in a mouse model]. *Klin Monbl Augenheilkd*. 2016;233:1313–1319.
37. Leckelt J, Guimaraes P, Kott A, Ruggeri A, Stachs O, Baltrusch S. Early detection of diabetic neuropathy by investigating CNFL and IENFD in thy1-YFP mice. *J Endocrinol*. 2016;231:147–157.

38. Melles GR, Ong TS, Ververs B, van der Wees J. Descemet membrane endothelial keratoplasty (DMEK). *Cornea*. 2006;25:987–990.
39. Melles GR, Wijdh RH, Nieuwendaal CP. A technique to excise the Descemet membrane from a recipient cornea (descemetorhexis). *Cornea*. 2004;23:286–288.
40. van Dijk K, Ham L, Tse WH, et al. Near complete visual recovery and refractive stability in modern corneal transplantation: Descemet membrane endothelial keratoplasty (DMEK). *Cont Lens Anterior Eye*. 2013;36:13–21.
41. Naumann GO, Schlotzer-Schrehardt U. Keratopathy in pseudoexfoliation syndrome as a cause of corneal endothelial decompensation: a clinicopathologic study. *Ophthalmology*. 2000;107:1111–1124.
42. Chen X, Nadiarynkh O, Plotnikov S, Campagnola PJ. Second harmonic generation microscopy for quantitative analysis of collagen fibrillar structure. *Nat Protoc*. 2012;7:654–669.
43. Michelacci YM. Collagens and proteoglycans of the corneal extracellular matrix. *Braz J Med Biol Res*. 2003;36:1037–1046.
44. Duggan MJ, Rose-Nussbaumer J, Lin CC, Austin A, Labadzinzki PC, Chamberlain WD. Corneal higher-order aberrations in Descemet membrane endothelial keratoplasty versus ultrathin DSAEK in the Descemet endothelial thickness comparison trial: a randomized clinical trial. *Ophthalmology*. 2019;126:946–957.
45. Wacker K, McLaren JW, Amin SR, Baratz KH, Patel SV. Corneal high-order aberrations and backscatter in Fuchs' endothelial corneal dystrophy. *Ophthalmology*. 2015;122:1645–1652.
46. Galgauskas S, Juodkaite G, Tutkuviene J. Age-related changes in central corneal thickness in normal eyes among the adult Lithuanian population. *Clin Interv Aging*. 2014;9:1145–1151.
47. Galgauskas S, Norvydaite D, Krasauskaite D, Stech S, Asoklis RS. Age-related changes in corneal thickness and endothelial characteristics. *Clin Interv Aging*. 2013;8:1445–1450.
48. Artym VV. Dense fibrillar collagen is a master activator of invadopodia. *Mol Cell Oncol*. 2016;3:e1035476.
49. Artym VV, Swatkoski S, Matsumoto K, et al. Dense fibrillar collagen is a potent inducer of invadopodia via a specific signaling network. *J Cell Biol*. 2015;208:331–350.
50. Provenzano PP, Inman DR, Eliceiri KW, et al. Collagen density promotes mammary tumor initiation and progression. *BMC Med*. 2008;6:11.
51. Garcerant D, Hirnschall N, Toalster N, Zhu M, Wen L, Moloney G. Descemet's stripping without endothelial keratoplasty. *Curr Opin Ophthalmol*. 2019;30:275–285.
52. Huang MJ, Kane S, Dhaliwal DK. Descemetorhexis without endothelial keratoplasty versus DMEK for treatment of Fuchs endothelial corneal dystrophy. *Cornea*. 2018;37:1479–1483.
53. Zygoura V, Baydoun L, Ham L, et al. Quarter-Descemet membrane endothelial keratoplasty (Quarter-DMEK) for Fuchs endothelial corneal dystrophy: 6 months clinical outcome. *Br J Ophthalmol*. 2018;102:1425–1430.
54. Tallot P, Grongnet JF, David JC. Dual perinatal and developmental expression of the small heat shock proteins [FC12]aB-crystallin and Hsp27 in different tissues of the developing piglet. *Biol Neonate*. 2003;83:281–288.
55. Wistow G. The human crystallin gene families. *Hum Genomics*. 2012;6:26.

Investigative Ophthalmology & Visual Science